Full Articles

Nature of weak inter- and intramolecular interactions in crystals
1. The F...O and F...H contacts in the crystal of 2-trifluoroacetyl-5-trifluoromethylpyrrole

K. A. Lyssenko and M. Yu. Antipin*

A. N. Nesmeyanov Institute of Organoelement Compounds, Russian Academy of Sciences, 28 ul. Vavilova, 119991 Moscow, Russian Federation. Fax: +7 (095) 135 5085. E-mail: kostya@xray.ineos.ac.ru

The topological analysis of the electron density distribution in the crystal of 2-trifluoroacetyl-5-trifluoromethylpyrrole revealed that the F...H and F...O intermolecular contacts correspond to attractive interactions. The energies of these interactions were estimated from the experimental data and it was shown that these contacts are similar to the C—H...O contacts. Analysis of the deformation electron density revealed that the F...O contacts correspond to transfer of the lone electron pair of a fluorine atom to the antibonding π-orbital of the C=O bond.

Key words: pyrrole derivatives with fluorine-containing substituents, C—H...F and F...O contacts, supramolecular chemistry, quantum-chemical calculations, electron density distribution, topological theory "Atoms in molecules," X-ray analysis.

Considerable interest in intermolecular contacts in the studies on crystalline organic, organoelement, and organometallic compounds is primarily due to the role played by such contacts in the formation of the supramolecular structure.[1] That is why revealing stable supramolecular synthons and structure-forming contacts and especially estimation of their energies have become central problems in the studies on polymorphism, spontaneous separation of enantiomers and in the search for "structure—property" relationships and design of materials with prescribed physicochemical characteristics.[1—5]

Most often, the presence of an intermolecular contact in structural studies is established based on analysis of geometric parameters only (more rigorously, based on comparison of the intermolecular distances with the sum of corresponding van der Waals radii[1,2]). Though such a geometric approach (especially its combination with statistical processing of data on the related intermolecular contacts using the Cambridge Structural Database) allows one to reveal the most stable supramolecular motifs and types of intermolecular contacts (see, *e.g.*, Ref. 6), it appears to be insufficient in the investigations of poorly studied weak interactions.[2]

In particular, this holds for contacts involving fluorine atoms, for which the known van der Waals radii make the range of distances so narrow that nearly completely ex-

Published in Russian in *Izvestiya Akademii Nauk. Seriya Khimicheskaya,* No. 1, pp. 11—18, January, 2004.

1066-5285/04/5301-0010

clude the possibility for any specific interaction to occur in the condensed state.[7] Besides, fluorine-containing (especially, fluoroalkyl) groups are often disordered in the crystal, which also hampers practical implementation of statistical methods of analysis to reveal stable intermolecular contacts.

Some examples of the C—H...F interactions have been reported;[8—13] however, their structure-forming role has been a debated topic (see Refs. 11, 14, and 15). As to the F...F, F...Hal, or F...chalcogen interactions, a number of authors cast some doubt on the possibility for them to occur in crystals.[7,11,16,17]

In addition to the geometric criteria, the use of X-ray diffraction data also permits unambiguous establishment of the presence of inter- and intramolecular interactions based on the topological analysis of the electron density distribution function ($\rho(\mathbf{r})$) in the framework of the theory "Atoms in molecules."[18,19] The key advantages of this approach are the possibility of answering the question "Does the shortened distance correspond to attractive interaction?" and estimating the energy of the contact using the potential energy density ($V(\mathbf{r})$) at the corresponding critical point (3, −1).[19,20]

Based on this, it was of interest to clarify the role of the intermolecular contacts involving fluorine atoms in the formation of the crystal structure and to compare the topological characteristics of such contacts with the corresponding characteristics of other weak contacts (*e.g.*, C—H...O). We analyzed the experimental electron density distribution in the crystal of 2-trifluoroacetyl-5-trifluoromethylpyrrole (**1**) at 130 K (Fig. 1). To assess the effect of the crystal packing on both the molecular geometry and peculiarities of the electron density distribution, we performed quantum-chemical calculations at the B3PW91/cc-pVDZ level.

Results and Discussion

Molecular geometry and crystal structure. The principal bond lengths and bond angles in the isolated molecule **1** and in the crystal are listed in Table 1. As can be seen, the computational method employed in this work provided an excellent agreement between the experimental and calculated geometric parameters.

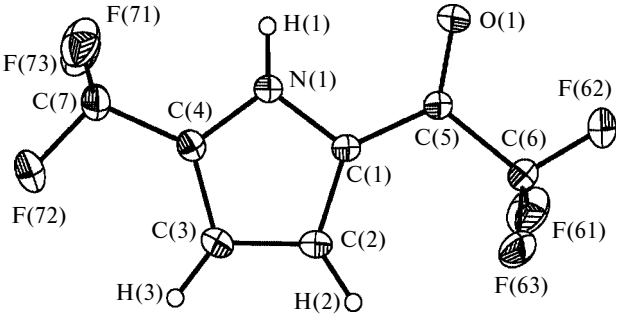

Fig. 1. Overall view of the molecule of compound **1** (non-hydrogen atoms are represented as probability ellipsoids (p = 50%) of thermal vibrations).

Table 1. Bond lengths (d), bond angles (ω), and parameters of the hydrogen bond N—H...O in the crystal and molecule of 2-trifluoroacetyl-5-trifluoromethylpyrrole and in its H-bonded dimer according to X-ray analysis data and results of quantum-chemical B3PW91/cc-pVDZ calculations

Parameter	Crystal	Molecule	H-bonded dimer
Bond		d/Å	
O(1)—C(5)	1.2192(9)	1.217	1.225
C(1)—N(1)	1.376(1)	1.372	1.375
N(1)—C(4)	1.351(1)	1.355	1.350
C(1)—C(2)	1.393(1)	1.391	1.395
C(1)—C(5)	1.438(1)	1.451	1.438
C(2)—C(3)	1.404(1)	1.407	1.401
C(3)—C(4)	1.387(1)	1.391	1.395
C(6)—F(61)	1.330(1)	1.347	1.346
C(6)—F(62)	1.330(1)	1.327	1.327
C(6)—F(63)	1.332(1)	1.347	1.346
C(7)—F(71)	1.332(1)	1.349	1.345
C(7)—F(72)	1.329(1)	1.338	1.342
C(7)—F(73)	1.337(1)	1.349	1.345
Angle		ω/deg	
C(4)—N(1)—C(1)	108.45(6)	109.5	108.9
N(1)—C(1)—C(2)	108.10(7)	107.7	107.8
N(1)—C(1)—C(5)	119.69(6)	118.2	120.4
C(2)—C(1)—C(5)	132.21(7)	134.2	131.7
O(1)—C(5)—C(1)	124.67(7)	123.1	125.0
O(1)—C(5)—C(6)	117.75(7)	120.2	118.2
C(1)—C(5)—C(6)	117.55(6)	116.7	116.8
F(62)—C(6)—F(61)	107.90(8)	108.5	108.5
F(62)—C(6)—F(63)	107.91(7)	108.5	108.5
F(61)—C(6)—F(63)	107.79(8)	107.4	107.6
F(72)—C(7)—F(71)	107.90(8)	108.0	107.9
F(72)—C(7)—F(73)	107.21(8)	108.0	107.9
F(71)—C(7)—F(73)	106.15(8)	106.4	107.1
Hydrogen bond N—H...O			
N(1)—H(1)*/Å	1.027	—	1.027
H(1)...O(1′)**/Å	1.855	—	1.819
N(1)...O(1′)/Å	2.860(1)	—	2.830
N(1)—H(1)...O(1′)/deg	165.3	—	167.4

* The N(1)—H(1) distance in the crystal was normalized to 1.027 Å according to B3PW91/cc-pVDZ calculations.

** The atom O(1′) was generated from the basis atom by the symmetry transformation $-x$, $1-y$, $1-z$.

The presence of a carbonyl group causes a substantial lengthening of the N(1)—C(1) bond compared to the corresponding values for the N(1)—C(4) bond (see Table 1). The difference between the N(1)—C(1) and N(1)—C(4) bond lengths (0.25 and 0.17 Å in the crystal and in the molecule, respectively) coincides with the average value of this parameter (0.24 Å), which was obtained by statistical averaging over a total of forty-three

ordered structures of pyrrole derivatives containing the carbonyl group in position 2 and an aliphatic carbon atom in position 5, retrieved from the Cambridge Structural Database.

Despite the presence of conjugation, the carbonyl group in molecule **1** is slightly rotated (the O(1)—C(5)—C(1)—N(1) torsion angle is 3.5°). An analogous distortion of the most preferable conformation is also observed for the trifluoromethyl groups. It is known[21] that, similarly to the methyl group, the trifluoromethyl group preferably adopts the synperiplanar conformation with respect to the double bond. This conformation in the case of Me group is so much more favorable that distortion of the synperiplanar conformation in *N*-methyl-2-pyrrolidone allowed[22] an unambiguous determination and estimation of the energy of the C—H...O intermolecular contacts.

The magnitudes of torsion angles in molecule **1** show the following. The CF_3 group in position 5 is only slightly rotated about the C(3)—C(4) double bond (the F(72)—C(7)—C(4)—C(3) angle is 2.1°), while for the CF_3 group linked to the carbonyl group the corresponding angle of rotation with respect to the C(5)=O(1) bond reaches 11.4°. Taking into account that, according to the calculations of isolated molecule **1**, the energy minimum corresponds to a C_s structure (both CF_3 groups adopt synperiplanar conformations with respect to the C=C and C=O bonds), we can suggest that this rotation is due to the crystal packing effect.

Noteworthy is that the synperiplanar arrangement of the CF_3 groups in the isolated molecule causes a strong distortion of their geometries, which manifests itself in shortening of the C(6)—F(62) and C(7)—F(72) bonds and in a systematic decrease in the bond angles involving those fluorine atoms that are in synclinal positions relative to the double bonds (see Table 1).

Though the N—H bond and the trifluoroacetyl group make the molecule a convenient building block for various supramolecular synthons (*e.g.*, helices, see Ref. 6), the most probable process is the formation of a centrosymmetric H-bonded dimer (N—H...O bond) as in the crystal structure of compound **1**. The length of the N(1)...O(1′) distance (2.860(1) Å, see Table 1) allows this hydrogen bond to be treated as a contact with intermediate energy. Hence, it can cause rotation of the carbonyl group as a result of weakening of conjugation.

To evaluate the effect of the N—H...O bond on the conformations of the CF_3 groups, we carried out B3PW91/cc-pVDZ calculations of the H-bonded dimer. This level of theory permitted an excellent reproduction of the experimental parameters of the hydrogen bond (namely, the N...O distance was 2.830 Å, see Table 1). Similarly to the monomer, the energy minimum also corresponds to the structure with C_s symmetry. The principal bond lengths in the H-bonded dimer remain virtually unchanged, except for the N—H bond, which is lengthened by 0.013 Å due to the formation of the hydrogen bond. It should also be noted that, similarly to the crystal, calculations of the H-bonded dimer revealed no variations of the bond angles and bond lengths in the CF_3 group linked to the C(4) atom.

Using the results of calculations of the H-bonded dimer and isolated molecule, we estimated the energy of the N—H...O hydrogen bond at 5.35 kcal mol^{-1} with inclusion of zero-point vibrational energy correction.

Thus, rotation of the CF_3 groups seems to be due to the intermolecular contacts formed by the fluorine atoms. Analysis of the crystal packing revealed that both CF_3 groups are involved in intermolecular interactions (Table 2). For instance, the F(72) atom forms a contact with the H(3′) atom, which permits the N—H...O-bonded dimers to be linked into stripes. As can be seen, a feature of the stripes is alternation of the ten-membered planar rings linked through the F...H and H...O hydrogen bonds. Therefore, the molecular graphs of these interactions are equivalent. In turn, the F(62)...H(2″) contacts formed by the trifluoroacetyl group link stripes to form layers (Fig. 2).

Besides the F...H contacts, the CF_3 group forms the F(73)...O(1″) contact responsible for cross-linking the layers into the three-dimensional cage (see Table 2 and Fig. 3).

Based on the fact that the geometric parameters of the H-bonded dimers in the crystal and in the free molecules are similar and taking into account the energy of the H-bonded dimer, it is reasonable to suggest that the N—H...O bonds will also remain in a saturated solution.

Table 2. Principal geometric parameters of the intermolecular contacts X—Y...F—C involving fluorine atoms in the crystal of compound **1**

X—Y...F—C	Symmetry transformation	Distance/Å		Angle/deg	
		X...F	Y...F*	X—Y—F	Y—F—C
C(2)—H(2)...F(62)—C(6)	$1 + x$, $3/2 - y$, $1/2 + z$	3.248(1)	2.50	126	152
C(3)—H(3)...F(72)—C(7)	$1 - x$, $2 - y$, $2 - z$	3.562(1)	2.54	158	164
C(5)—O(1)...F(73)—C(7)	$1 - x$, $1 - y$, $1 - z$	4.156(1)	2.897(2)	93.0(1)	156.4(1)

* The C—H distances were normalized to 1.07 Å.

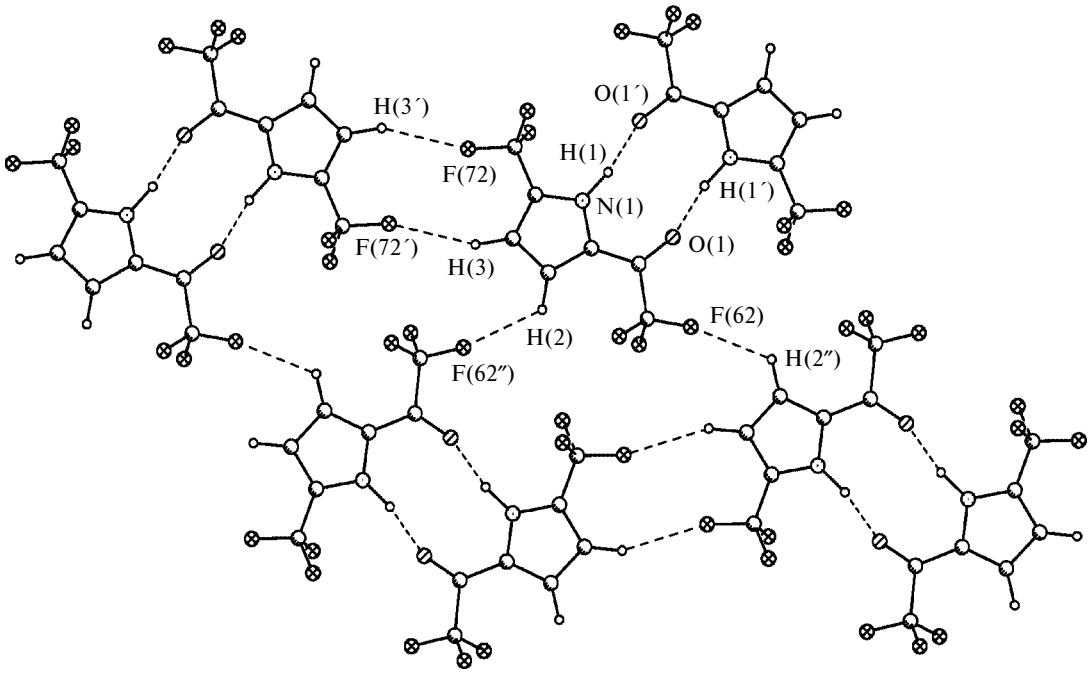

Fig. 2. Scheme illustrating the formation of the N—H...O- and C—F...H-bonded layers in the crystal of **1**.

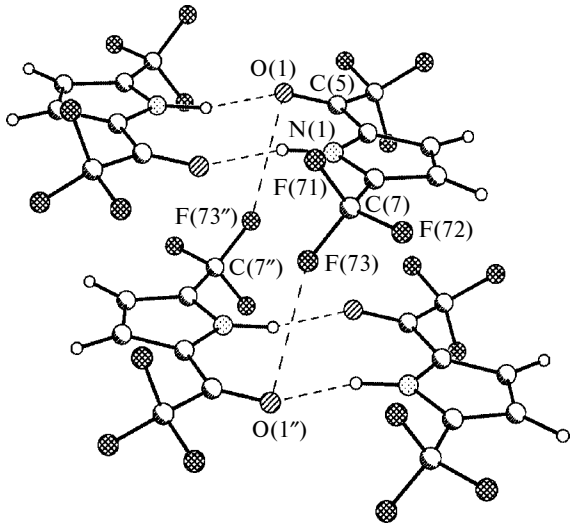

Fig. 3. Scheme illustrating the formation of the contacts F...O in the crystal of **1**.

Therefore, the weak contacts F...H and F...O rather than the N—H...O bonds seem to be the main structure-forming contacts in the case of a growing crystal.

To assess whether or not do the contacts involving fluorine atoms (especially, the F...O contact) belong to attractive interactions, we carried out the topological analysis of the electron density distribution function ($\rho(\mathbf{r})$) in the crystal of compound **1**. The analytical form of the static electron density distribution function was obtained by the multipole refinement of the data of X-ray diffraction study (see Experimental).

Topological analysis of the electron density distribution function. Prior to reporting the results of topological analysis of the electron density distribution, we will consider some features of the deformation electron density (DED) distribution in the region of the N—H...O, C—H...F, and C—O...F contacts.

Surprisingly, a comparison of the DED distribution for the intermolecular interactions revealed in the crystal of compound **1** showed that, in spite of the clearly seen energy difference between these interactions, the character of accumulation of the electron density in the region of the C—H...F and N—H...O contacts is virtually identical to that in the promolecule (Fig. 4). The salient features of the DED distribution (polarization of the lone electron pairs, LEP, and electron depletion in the region of the hydrogen bond) also persists for the F(62)...H(2) contact. Yet another feature of the DED distribution in the vicinity of the O(1) atom (see Fig. 4, *a*) is nonequivalence of the LEP of the O(1) atom, which can be due to both conjugation between one of them with the π-system of pyrrole and to the influence of the hydrogen bond. It should also be noted that a substantial decrease in the DED in the region of the C—F bond is primarily due to the so-called electron density "overresidue" effect (see, *e.g.*, Ref. 23) rather than the decrease in the covalent component.

In contrast to the hydrogen bonds, the character of the DED distribution in the region of the F...O contact is to be clarified. According to the published data, almost all F...O interactions can be described in the framework of the "peak—hole" model (see, *e.g.*, Ref. 24). However, in

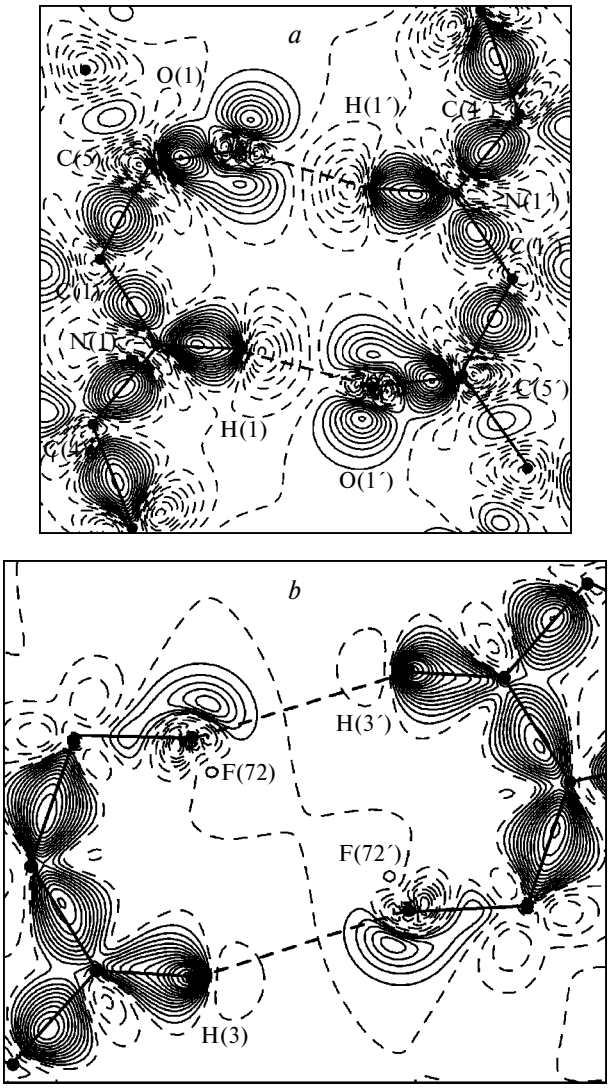

Fig. 4. Section of the DED in the region of ten-membered rings linked through the H...O (*a*) and F...H (*b*) contacts. The maps are contoured at intervals of 0.05 e Å^{-3}. The negative values are shown by dashed lines.

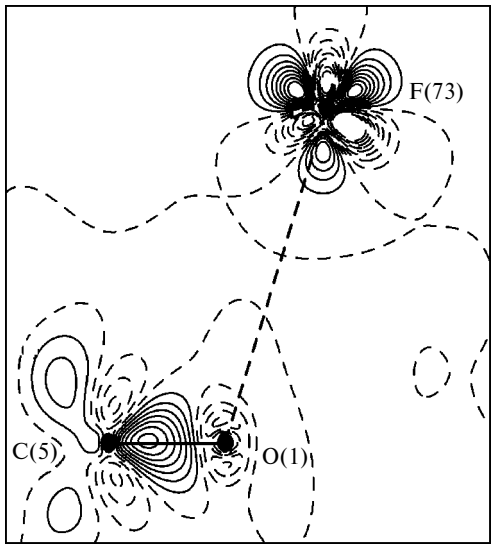

Fig. 5. Section of the DED in the region of the contact C=O...F in the molecule of **1**. The maps are contoured at intervals of 0.1 e Å^{-3}; the negative values are shown by dashed lines.

this case the DED maximum can correspond to both the LEP (n-orbital) of the fluorine atom and the LEP of the O atom of the carbonyl group. Based on the values of geometric parameters, this contact can correspond to two directions of charge transfer, n_O—σ*(C—F) and n_F—π*(CO). However, the shape of the DED section in the plane passing through the C(5), O(1), and F(73) atoms (Fig. 5) indicates polarization of the LEP of the fluorine atom toward the region of electron depletion in the vicinity of the O(1) atom. Hence, charge transfer occurs from the F atom to the carbonyl group rather than in the opposite direction. Because the n-orbital of the F(73) atom is directed nearly perpendicular to the C=O bond, we can suggest that this contact corresponds to the n_F—π*(CO) interaction and, hence, it can also be responsible for nonequivalence of the LEP of the O(1) atom (see Fig. 4, *a*).

To assess the possibility of treating the intermolecular contacts described above as attractive interactions and to obtain semiquantitative estimates of their energies, we performed the topological analysis of the electron density distribution and the potential energy density.

Calculations of $V(\mathbf{r})$ were carried out using an approximation in the framework of the Thomas—Fermi theory.[25] Here, the kinetic energy density, $G(\mathbf{r})$, can be obtained from the following expression:

$$G(\mathbf{r}) = (3/10)(3\pi^2)^{2/3}[\rho(\mathbf{r})]^{5/3} + \\ + (1/72)|\nabla\rho(\mathbf{r})|^2/\rho(\mathbf{r}) + 1/6\nabla^2\rho(\mathbf{r}), \quad (1)$$

which in combination with the local expression of the virial theorem[18]

$$2G(\mathbf{r}) + V(\mathbf{r}) = 1/4\nabla^2\rho(\mathbf{r}) \quad (2)$$

allows both the potential energy density and the local energy density, $H_e(\mathbf{r})$, be calculated. This is of prime importance for correct determination of the type of the interatomic interaction.[18]

Search for critical points of the electron density and potential energy density (more exactly, $-V(\mathbf{r})$) functions showed that the chahacteristic set of critical points includes both the critical point (3, −1) for all expected chemical bonds (C—C, C—F, C=O, C—H, and N—C) and the critical point (3, −1) located in the regions of the N...H, F...H, and F...O contacts. Based on the Poincare—Hopf relationship, these interactions cause the formation of additional rings, which manifests itself as the appearance of a critical point (3, +1) corresponding to

the five-membered pyrrole ring and to ten-membered H-bonded rings. We also localized the critical points (3, +1) corresponding to large rings that are formed upon linkage of stripes, as well as polyhedral critical points (3, +3) corresponding to cross-linking of layers into the three-dimensional cage. However, the components of the curvature are close to zero, which hampers unambiguous attribution of these critical points to a particular type based on the sum of the signs of the eigenvalues (signature) of the Hessian matrix.

Coincidence of the chahacteristic sets for the potential energy density and electron density functions should be pointed out. This unambiguously points that all contacts for which some bond pathways are observed (this is equivalent to the presence of the critical point (3, −1)) correspond to attractive interactions.[18b]

The topological characteristics of the C—C, C—N, and C=O bonds at the critical point (3, −1) of the function $\rho(\mathbf{r})$, including the ellipticities (ε), obtained by the multipole refinement and using the results of quantum-chemical calculations of the H-bonded dimer are close to one another. All these bonds correspond to the shared type of interatomic interaction (negative electron density Laplacian, $\nabla^2\rho(\mathbf{r})$, at the critical point (3, −1)). It should be noted that the electron densities and ε values in the pyrrole ring are rather close, being in good agreement with the aromaticity of this ring. For instance, the $\rho(\mathbf{r})$ and ε values at the critical point (3, −1) in the crystal vary in the ranges 1.99—2.24 e Å^{-3} and 0.17—0.27, respectively (*cf.* 2.01—2.15 e Å^{-3} and 0.18—0.30, respectively, for the H-bonded dimer). The corresponding parameters for the C(5)—C(6) bond are 1.63 e Å^{-3} and 0.07 (crystal) and 1.71 e Å^{-3} and 0.04 (H-bonded dimer), which is much smaller than in the pyrrole ring.

The shared type of interaction is also observed for the polar bonds C—F; however, here the differences between the $\nabla^2\rho(\mathbf{r})$ and $\rho(\mathbf{r})$ values are somewhat larger. In particular, the $\rho(\mathbf{r})$ and $\nabla^2\rho(\mathbf{r})$ magnitudes at the critical point (3, −1) of the C—F bonds respectively vary within the following limits: 1.74—2.07 e Å^{-3} and −18.55——6.06 e Å^{-5} (multipole refinement) and 1.81—1.90 e Å^{-3} and −9.30——8.36 e Å^{-5} (B3PW91/cc-ppvDZ calculations). This can be a consequence of the difference between the bond lengths, influence of the F...H and F...O contacts, and a rather low accuracy in determining the components of the curvature in the vicinity of the critical point (3, −1) for a given type of bond.[26] However, it should be noted that the quantum-chemically calculated magnitude and even (in some cases) sign of $\nabla^2\rho(\mathbf{r})$ at the critical points (3, −1) of the C—F bonds the depend not only on the basis set employed but also on the method of inclusion of electron correlation.[27] Therefore, in this case a comparison of the experimental data and the results of quantum-chemical calculations is somewhat ambiguous. As far as we know, the one and only example for comparison available to date is provided by pentafluorobenzoic acid.[26] Namely, the multipole refined experimental $\rho(\mathbf{r})$ and $\nabla^2\rho(\mathbf{r})$ values for the C—F bonds in the crystal of this compound lie between 2.00—2.12 e Å^{-3} and −21.8——25.2 e Å^{-5}, respectively.

Unlike the above-mentioned C—C, C—F, C=O, C—H, and N—H bonds, the F...H, F...O, and H...O contacts are characterized by positive $\nabla^2\rho(\mathbf{r})$ values at the critical point (3, −1). Though the low values of $\rho(\mathbf{r})$ and $\nabla^2\rho(\mathbf{r})$ in the case of the contacts involving fluorine atoms unambiguously allow their attribution to the closed-shell interactions[18a] (Table 3), for this conclusion for the N—H...O bond is not obvious. Earlier, we have shown that intramolecular hydrogen bonds in 3-acetyl-4-hydroxycoumarin[20b] and tetraacetylethylene[28] and the intermolecular hydrogen bond in diphenylphosphonic acid[29] correspond to an intermediate type of interactions, which is characterized by negative local density energy at the critical point (3, −1) despite a positive value of $\nabla^2\rho(\mathbf{r})$ at that point.

To evaluate $H_e(\mathbf{r})$, we used the above-mentioned approximation for the kinetic energy density (Eq. (1)). The calculated values of $G(\mathbf{r})$, $V(\mathbf{r})$ and $H_e(\mathbf{r})$ are listed in

Table 3. Topological characteristics of intermolecular contacts in the crystal of compound **1**

Contact	$\rho(\mathbf{r})$/e Å^{-3}	$\nabla^2\rho(\mathbf{r})$/e Å^{-5}	$G(\mathbf{r})$	$V(\mathbf{r})$	$H_e(\mathbf{r})$	E_{cont} /kcal mol^{-1}
			a.u.			
N—H...O	0.1180, 0.203 [a]	3.770, 2.839	0.0295, 0.0254	−0.0198, −0.0223	0.0096, 0.0036	6.21, 7.00
C(5)—O(1)...F(73)[b]	0.0450	0.82	0.0064	−0.0042	0.0022	1.31
C(2)—H(2)...F(62)[c]	0.0420	0.67	0.0052	−0.0035	0.0017	1.09
C(3)—H(3)...F(72)[d]	0.0170	0.44	0.0032	−0.0018	0.0014	0.56

[a] Obtained for the N—H...O bond in the H-bonded dimer (B3PW91/cc-pVDZ calculations).
[b] The atom was generated from the basis atom by the symmetry transformation $1-x, 1-y, 1-z$.
[c] The atom was generated from the basis atom by the symmetry transformation $1+x, 3/2-y, 1/2+z$.
[d] The atom was generated from the basis atom by the symmetry transformation $1-x, 2-y, 2-z$.

Table 3 from which it can be seen that both the relatively strong N—H...O bond and the weak contacts C—H...F and F...O belong to closed-shell interactions.

It should be noted that, in spite of the close geometric parameters of the N—H...O bond in the crystal and in the gas phase, the topological characteristics at the critical point (3, −1) obtained from multipole refinement and from quantum-chemical calculations appreciably differ. The weakening of the hydrogen bond is probably due to both the crystal field effect and ignoring the effect of the F...O contact in quantum-chemical calculations of the H-bonded dimer.

According to the published data, the potential energy density for closed-shell interactions is related to the contact energy (E_{cont}).[20] Earlier, the relationship $E_{cont} = -1/2V(\mathbf{r})$ gave an exact quantitative estimate of the interaction energy for the C—H...O contacts;[20a] however, further studies disclosed that sometimes this approximation is impossible to correctly reproduce the interaction energies obtained from more rigorous quantum-chemical calculations.[29] For instance, Table 3 shows that the N—H...O bond energy calculated using this relationship substantially overestimates the energy obtained from quantum-chemical calculations.

At present, there is no commonly accepted correlation scheme of assessing the interaction energy; nevertheless, comparison of the E_{cont} values expressed in units of the potential energy density allows the order of the contact energies to be correctly reproduced at a qualitative level.[20] Therefore, though the absolute value of E_{cont} (for, *e.g.*, calculating the crystal lattice energy) cannot be obtained as yet, semiquantitative estimates suitable for comparing interactions of different nature are arranged in a correct order.

Based on this, we compared the energies of the title contacts using the relation mentioned above, $E_{cont} = -1/2V(\mathbf{r})$.[20] As can be seen from the data in Table 3, the energy of the C—F...O interaction, expressed in units of the potential energy, is much higher than that of the C—H...F interactions, being comparable with the C—H...O contacts characterized by a H...O distance of about 2.3 Å.[29,30] In the same sense the C—H...F contacts are comparable with the weak contacts C—H...O characterized by the H...O distances longer than 2.5 Å.[20b,30]

It should be noted that, despite their low energies, these interactions can and do have a strong effect not only on the formation of the crystal packing but also on the molecular dynamics in crystals, which was earlier exemplified by intramolecular proton transfer in the crystals of 3-acetyl-4-hydroxycoumarin[20b] and tetraacetylethylene.[29]

Thus, our X-ray study of the electron density distribution in the crystal of 2-trifluoroacetyl-5-trifluoromethylpyrrole showed that the contacts involving fluorine atoms significantly affect the formation of the crystal structure while their energies are comparable with the energies of the intermediate and weak C—H...O contacts.

Taking into account that heterocyclic compounds containing fluorinated substituents possess a high biological activity, the results obtained in this work as well as systematic studies on the electron density distribution in the crystal can provide a rich source of additional information on the role of the interactions involving fluorine atoms in the metabolism of this class of compounds.

Experimental

X-ray diffraction study of compound **1** ($C_7H_3F_6NO$) was carried out on a Siemens P3/PC automatic four-circle diffractometer (Mo-Kα radiation, graphite monochromator, θ/2θ scan, $2\theta_{max} \le 82°$) at $T = 130$ K. At this temperature, the crystals are monoclinic: $a = 4.994(1)$ Å, $b = 17.019(4)$ Å, $c = 9.753(3)$ Å, $\beta = 97.72°$, $V = 821.4(4)$ Å^3, $d_{calc} = 1.869$ g cm^{-3}, $M = 231.10$, $F(000) = 456$, $\mu = 2.16$ cm^{-1}, $Z = 4$ ($Z' = 1$), and the space group is $P2_1/c$. Out of 5777 measured reflections, a total of 5369 independent reflections were included in the calculations and refinement ($R_{int} = 0.0196$). The structure was solved by the direct method and refined using the full-matrix least-squares method in the full-matrix anisotropic approximation based on F^2_{hkl}. Hydrogen atoms were located from the difference electron density maps and were included in the refinement with isotropic thermal parameters. The final reliability factors were as follows: $R = 0.0472$ based on a total of 3629 reflections with $I > 2\sigma(I)$, $wR_2 = 0.1223$, and GOF = 1.002 based on all reflections. All calculations were carried out on an IBM PC AT using the SHELXTL PLUS software.

To obtain the analytical form of the experimental electron density function, a multipole refinement of the X-ray diffraction data was performed in the framework of the Hansen—Coppens model[31] using the XD program complex.[32] The multipole refinement of all non-hydrogen atoms included refinement of the coordinates, anisotropic thermal parameters, and multipole parameters up to the octupole level ($l = 3$) without symmetry restrictions. Positions of hydrogen atoms and their isotropic thermal parameters were not refined. Before the refinement, the C—H and N—H distances were normalized to the "ideal" neutron diffraction values (1.07 and 1.027 Å, respectively). The hydrogen atoms were refined up to the dipole level ($l = 1$) with inclusion of cylindrical symmetry. Correctness of the calculated anisotropic parameters of atomic displacements was estimated using Hirshfeld´s test,[33] which for bonds (including the C—F bonds) was at most $10 \cdot 10^{-4}$ Å^2. The multipole refinement converged to $R = 0.0316$, $wR = 0.0289$, and GOF = 0.93. The electron density maxima in the residual electron density maps, $(\rho(\mathbf{r})_{exp} - \rho(\mathbf{r})_{mult})$, were no higher than 0.10 e Å^{-3}.

All calculations were carried out with full geometry optimization using the B3PW91 hybrid functional, the cc-pVDZ basis set, and the Gaussian98W program[34] with the parameters Opt = Vtight, Grid(UltraFine). For correct estimation of the energy of the hydrogen bond, the optimization was followed by vibrational frequency calculations. The topology of the theoretical (calculated) electron density distribution was analyzed using the EXTREME programs.[35]

This work was financially supported by the Russian Foundation for Basic Research (Project No. 03-03-32214) and by the Presidential Grants for support of leading scientific schools (NSh 1060.2003.30) and young Ph.D. researchers (MK-1209.2003.03).

References

1. G. R. Desiraju and T. Steiner, *The Weak Hydrogen Bond in Structural Chemistry and Biology*, Oxford Sci. Publ., Oxford, 1999; G. R. Desiraju, *J. Chem. Soc.*, *Dalton Trans.*, 2000, 3745.
2. G. R. Desiraju, *Acc. Chem. Res.*, 2002, **35**, 565.
3. T. Steiner, *Angew. Chem.*, *Int. Ed. Engl.*, 2002, **41**, 48.
4. E. A. Meyer, R. K. Castellano, and F. Diederich, *Angew. Chem.*, *Int. Ed. Engl.*, 2003, **42**, 1210.
5. L. Pérez-García and D. B. Amabilino, *Chem. Soc. Rev.*, 2002, **31**, 342.
6. F. H. Allen, W. D. S. Motherwell, P. R. Raithby, G. P. Shields, and R. Taylor, *New. J. Chem.*, 1999, 25.
7. R. S. Rowland and R. Taylor, *J. Phys. Chem.*, 1996, **100**, 7384.
8. P. Murray-Rust, W. C. Stallings, C. T. Monti, R. K. Preston, and J. P. Glusker, *J. Am. Chem. Soc.*, 1983, **105**, 3206.
9. L. Shimoni, H. L. Carrell, J. P. Glusker, and M. M. Coombs, *J. Am. Chem. Soc.*, 1994, **116**, 8162.
10. K. A. Lyssenko, M. Y. Antipin, and V. N. Lebedev, *Inorg. Chem.*, 1998, **37**, 5834.
11. V. R. Thalladi, H.-C. Weiss, D. Bläser, R. Boese, A. Nabgia, and G. R. Desiraju, *J. Am. Chem. Soc.*, 1998, **120**, 8702.
12. H. Lee, C. B. Knobler, and M. F. Hawthorne, *Chem. Commun.*, 2000, 2485.
13. F. Grepioni, G. Cojazzi, S. M. Draper, N. Scully, and D. Braga, *Organometallics*, 1998, **17**, 296.
14. J. A. K. Howard, V. J. Hoy, D. Hagan, and G. T. Smith, *Tetrahedron*, 1996, **52**, 12613.
15. J. D. Dunitz and R. Taylor, *Chem. Eur. J.*, 1997, **3**, 89.
16. Yu. V. Zefirov and P. M. Zorkii, *Usp. Khim,*, 1995, **64**, 446 [*Russ. Chem. Rev.*, 1995, **64**, 415 (Engl. Transl.)].
17. J. P. M. Lommerse, A. J. Stone, R. Taylor, and F. H. Allen, *J. Am. Chem. Soc.*, 1996, **118**, 3108.
18. (a) R. F. W. Bader, *Atoms in Molecules. A Quantum Theory*, Clarendron Press, Oxford, 1990; (b) R. F. W. Bader, *J. Chem. Phys.*, 1998, **A102**, 7314.
19. (a) V. G. Tsirelson and R. P. Ozerov, *Electron Density and Bonding in Crystals*, IOP, Bristol—Philadelphia, 1996; (b) T. S. Koritsánszky and P. Coppens, *Chem. Rev.*, 2001, **101**, 1583.
20. (a) E. Espinosa, E. Mollins, and C. Lecomte, *Chem. Phys. Lett.*, 1998, **285**, 170; (b) K. A. Lyssenko and M. Yu. Antipin, *Izv. Akad. Nauk*, *Ser. Khim.*, 2001, 400 [*Russ. Chem. Bull.*, *Int. Ed.*, 2001, **50**, 418]; (c) C. Gatti, E. May, and F. Cargnoni, *J. Phys. Chem. A*, 2002, **106**, 2707.
21. R. Benassi and F. Taddei, *J. Mol. Struct. (Theochem.)*, 1998, **430**, 113.
22. G. Müller, M. Lutz, and S. Harder, *Acta Crystallogr.*, *Sect. B*, 1996, **52**, 1014.
23. K. A. Lyssenko, M. Yu. Antipin, and V. N. Khrustalev, *Izv. Akad. Nauk*, *Ser. Khim.*, 2001, 1465 [*Russ. Chem. Bull.*, *Int. Ed.*, 2001, **50**, 1539].
24. W. Scherer, M. Spiegler, M. Tafipolsky, W. Hieringer, B. Reinhard, A. J. Downs, and G. S. McGrady, *Chem. Commun.*, 2000, 635.
25. D. A. Kirzhnitz, *Zh. Eksp. Teor. Fiz.*, 1957, **5**, 64 [*J. Exp. Theor. Phys.*, 1957, **5**, 64 (Engl. Transl.)].
26. A. Bach, D. Lentz, and P. Luger, *J. Phys. Chem.*, 2001, **105**, 7405.
27. J. Wang, B. G. Johnson, R. J. Boyd, and L. A. Eriksson, *J. Phys. Chem.*, 1996, **100**, 6317.
28. K. A. Lyssenko, D. V. Lyubetsky, and M. Yu. Antipin, *Mendeleev Commun.*, 2003, 60.
29. K. A. Lyssenko, G. V. Grintselev-Knyazev, and M. Yu. Antipin, *Mendeleev Commun.*, 2002, 128.
30. C. Gatti, E. May, R. Destro, and F. Cargnoni, *J. Phys. Chem.*, *A*, 2002, **106**, 2707.
31. N. K. Hansen and P. Coppens, *Acta Crystallogr.*, *Sect. A*, 1978, **34**, 909.
32. T. Koritsánszky, S. T. Howard, T. Richter, P. R. Mallinson, Z. W. Su, and N. K. Hansen, *XD* — A *Computer Program Package for Multipole Refinement and Analysis of Charge Densities from X-ray Diffraction Data*, IUCr, 1995.
33. F. L. Hirshfeld, *Acta Crystallogr.*, *Sect. A*, 1976, **32**, 239.
34. M. J. Frisch, G. W. Trucks, H. B. Schlegel, G. E. Scuseria, M. A. Robb, J. R. Cheeseman, V. G. Zakrzewski, J. A. Montgomery, Jr., R. E. Stratmann, J. C. Burant, S. Dapprich, J. M. Millam, A. D. Daniels, K. N. Kudin, M. C. Strain, O. Farkas, J. Tomasi, V. Barone, M. Cossi, R. Cammi, B. Mennucci, C. Pomelli, C. Adamo, S. Clifford, J. Ochterski, G. A. Petersson, P. Y. Ayala, Q. Cui, K. Morokuma, D. K. Malick, A. D. Rabuck, K. Raghavachari, J. B. Foresman, J. Cioslowski, J. V. Ortiz, A. G. Baboul, B. B. Stefanov, G. Liu, A. Liashenko, P. Piskorz, I. Komaromi, R. Gomperts, R. L. Martin, D. J. Fox, T. Keith, M. A. Al-Laham, C. Y. Peng, A. Nanayakkara, M. Challacombe, P. M. W. Gill, B. Johnson, W. Chen, M. W. Wong, J. L. Andres, C. Gonzalez, M. Head-Gordon, E. S. Replogle, and J. A. Pople, *Gaussian 98*, *Revision A.7*, Gaussian, Inc., Pittsburgh (PA), 1998.
35. J. Cheeseman, T. A. Keith, and R. W. F. Bader, *AIMPAC Program Package*, McMaster University, Hamilton (Ontario), 1992.

Received August 11, 2003;
in revised form October 17, 2003